



| | |
|------------------|--|
| Title | cDNA-based gene mapping and GC3 profiling in the soft-shelled turtle suggest a chromosomal size-dependent GC bias shared by sauropsids |
| Author(s) | Kuraku, Shigehiro; Ishijima, Junko; Nishida-Umehara, Chizuko; Agata, Kiyokazu; Kuratani, Shigeru; Matsuda, Yoichi |
| Citation | Chromosome Research, 14(2), 187-202 https://doi.org/10.1007/s10577-006-1035-8 |
| Issue Date | 2006-03 |
| Doc URL | http://hdl.handle.net/2115/30289 |
| Rights | The original publication is available at www.springerlink.com |
| Type | article (author version) |
| File Information | CR14-2.pdf |



[Instructions for use](#)

cDNA-based gene mapping and GC₃ profiling in the soft-shelled turtle suggests a chromosomal size-dependent GC bias shared by sauropsids.

Shigehiro Kuraku,^{1*} Junko Ishijima,² Chizuko Nishida-Umehara,^{2,3} Kiyokazu Agata,^{4,5} Shigeru Kuratani,¹ and Yoichi Matsuda^{2,3}

¹*Laboratory for Evolutionary Morphology, RIKEN Center for Developmental Biology, 2-2-3 Minatogima-minamimachi, Chuo-ku, Kobe 650-0047, Japan; Tel: +81-78-3063064; Fax: +81-78-3063370; E-mail: venezia@cdb.riken.jp;* ²*Laboratory of Animal Cytogenetics, Division of Genome Dynamics, Creative Research Initiative “Sousei”, Hokkaido University, North 10 West 8, Kita-ku, Sapporo 060-0810, Japan;* ³*Division of Biological Sciences, Graduate School of Science, Hokkaido University, Sapporo, 060-0810, Japan;* ⁴*Laboratory for Evolutionary Regeneration Biology, RIKEN Center for Developmental Biology, 2-2-3 Minatogima-minamimachi, Chuo-ku, Kobe, 650-0047, Japan*

**Correspondence.*

⁵*Present address: Laboratory for Molecular Developmental Biology, Department of Biophysics, Graduate School of Science, Kyoto University, Kyoto, 606-8502, Japan*

Running title: GC heterogeneity in the turtle genome

Key words: GC-content, sauropsida, turtle, microchromosome.

Abstract

Mammalian and avian genomes comprise several classes of chromosomal segments that vary dramatically in GC-content. Especially in chicken, microchromosomes exhibit a higher GC-content and a higher gene density than macrochromosomes. To understand the evolutionary history of the intra-genome GC heterogeneity in amniotes, it is necessary to examine the equivalence of this GC heterogeneity at the nucleotide level between these animals including reptiles, from which birds diverged. We isolated cDNAs for 39 protein-coding genes from the Chinese soft-shelled turtle, *Pelodiscus sinensis*, and performed chromosome mapping of 31 genes. The GC-content of exonic third positions (GC_3) of *P. sinensis* genes showed a heterogeneous distribution, and exhibited a significant positive correlation with that of chicken and human orthologs, indicating that the last common ancestor of extant amniotes had already established a GC-compartmentalized genomic structure. Furthermore, chromosome mapping in *P. sinensis* revealed that microchromosomes tend to contain more GC-rich genes than GC-poor genes, as in chicken. These results illustrate two modes of genome evolution in amniotes: mammals sophisticated the genomic configuration in which GC-rich and GC-poor regions coexist in individual chromosomes, whereas sauropsids (reptiles and birds) refined the chromosomal size-dependent GC compartmentalization in which GC-rich genomic fractions tend to be confined to microchromosomes.

Introduction

Mammalian and avian genomes have been revealed, by means of chromosome banding and density gradient centrifugations, to be composed of several classes of chromosomal segments that differ in GC-content, which are called ‘isochores’ (Bernardi *et al.* 1985). Although the evolutionary origin and intrinsic nature of this GC heterogeneity is not fully understood (Eyre-Walker & Hurst 2001), the existence of intra-genome GC heterogeneity was recently confirmed by analyses of whole-genome sequences in the chicken as well as human, mouse and rat (International Human Genome Sequence Consortium [IHGSC] 2001; Mouse Genome Sequencing Consortium [MGSC] 2002; International Chicken Genome Sequencing Consortium [ICGSC] 2004; Rat Genome Sequencing Project Consortium [RGSPC] 2004; also see Figure 1a).

Karyotypes of extant sauropsids (reptiles and birds) generally consist of two major components: macrochromosomes and microchromosomes (Burt 2002; Norris *et al.* 2004). In chicken, cytogenetic observations indicate that microchromosomes exhibit a higher gene density (McQueen *et al.* 1998; Smith *et al.* 2000), a higher density of CpG islands (McQueen *et al.* 1996) and a higher GC-content than macrochromosomes (Auer *et al.* 1987; Andreozzi *et al.* 2001). The whole genomic sequence of chicken has yielded trends consistent with the above, and, especially, suggested that the global GC-content of chromosomes increases exponentially with the reduction in chromosomal size (ICGSC 2004; also see Figure 1b), whereas this tendency is not seen in mammals and teleosts (Figures 1c-e). These features of the chicken genome suggest that avian microchromosomes might be the counterparts of mammalian GC-rich chromosomal segments (Andreozzi *et al.* 2001). However, it is not clear whether the intra-genome GC

heterogeneity observed in mammals and birds was derived from a common ancestor, or was the result of a convergence that occurred independently in the two lineages. Reptiles could provide valuable information for addressing this question.

The existence of intra-genomic GC heterogeneity in reptiles has not been fully confirmed by chromosome banding studies (Holmquist 1989) and density gradient centrifugation (Thiery *et al.* 1976; Hughes *et al.* 2002). However, some recent studies at the nucleotide level suggest that GC heterogeneity exists in reptilian genomes, based on variations in GC-contents in exonic third positions (GC₃) and introns of a limited number of genes (Hughes *et al.* 1999; Belle *et al.* 2002; Hamada *et al.* 2003). Here, the GC₃ of a gene is expected to positively correlate with the GC₃ of the genomic region where the gene is located, as confirmed in mammalian and avian genomes (Clay *et al.* 1996; Musto *et al.* 1999). However, the paucity of sequence information on reptilian species has inhibited understanding of the physical configuration of reptilian genomes and the evolutionary origin of heterogeneity in base composition.

In this study, we cloned and sequenced cDNAs of protein-coding genes from the Chinese soft-shelled turtle, *Pelodiscus sinensis*, and localized them to chromosomes by fluorescent *in situ* hybridization (FISH). The physical evidence of chromosomal configurations in the turtle, as suggested by cDNA-based approaches and comparison with chromosomal configurations in other amniotes, has highlighted two modes of genome evolution in amniotes.

Materials and methods

Isolation and sequencing of cDNAs with degenerate primers

Total RNA isolated from whole embryos of stage 14 *P. sinensis* was reverse transcribed into cDNA using an oligo(dT) primer and SuperScript III (Invitrogen). These cDNAs were used as templates for PCR amplification with the FastStart High Fidelity PCR System (Roche). The sense and antisense degenerate primers were designed based on the conserved amino acid residues in the multiple alignments constructed as described below, and are as shown in Table 1. PCR was conducted as follows: 2 min denaturation step at 94 °C; then 10 cycles of 94 °C for 15 s, 48 °C for 30 s, and 72 °C for 2 min; followed by 30 cycles of 94 °C for 15 s, 56 °C for 30 s, and 72 °C for 2 min. Modifications were made when required, depending on the presumed length of amplicons and the T_m value of the primers used. The PCR products were purified using MinElute (Qiagen) and cloned into a pT7Blue vector (Novagen). More than three independent clones per gene were sequenced using a 3100 Genetic Analyzer or 3730XL DNA Analyzer (Applied Biosystems). Upstream and downstream regions of isolated cDNAs were cloned and sequenced by 5' and 3' rapid amplification of cDNA ends (Frohman *et al.* 1988).

Estimation of numbers of synonymous and non-synonymous substitutions

Nucleotide sequences of orthologous gene pairs of chicken-turtle were manually aligned on the XCED program (Kato *et al.* 2002) based on alignments of the amino acid sequences of the proteins they encode. K_s and K_a were calculated with the codon-based maximum-likelihood method (Goldman & Yang 1994) and with the method of Nei and Gojobori (1986). Computations were processed using a PAML 3.1 package (Yang

1997).

Calculation of GC-content

cDNA sequences for human, mouse, rat, chicken, tiger pufferfish (*F. rubripes*), *C. intestinalis*, *Drosophila melanogaster* and *Caenorhabditis elegans* were downloaded from Ensembl (version 34 - Oct, 2005; URL: <http://www.ensembl.org/>; Hubbard *et al.* 2005). Those for sheep (*O. aries*), axolotl (*Ambystoma mexicanum*), *X. tropicalis*, zebrafish (*D. rerio*), and amphioxus (*Branchiostoma belcheri*) were downloaded from GenBank (version 148.0). After redundant sequences, which are thought to be derived from a single gene, has been assembled with Phrap (URL: <http://www.phrap.com/>), GC₃ and GC₄ were calculated using a Perl script with the bioperl module (Stajich *et al.* 2002). The calculation was automatically processed based on the open reading frame identified with a pairwise alignment between translated nucleotide sequences and corresponding amino acid sequences with BLASTX (Altschul *et al.* 1997). Analysis of variance (ANOVA) for statistical analysis of similarities in distribution of GC-contents was conducted with non-parametric rank tests on the assumption that the overall distribution of GC₃ for all the genes in one species does not have a normal distribution.

Chromosome preparation and FISH

Fibroblast cells derived from embryos of *P. sinensis* were cultured and used for chromosome preparations. Preparation of R-banded chromosomes and FISH were performed as described previously (Matsuda & Chapman 1995; Suzuki *et al.* 1999).

5-bromodeoxyuridine (BrdU) was incorporated into chromosomes during the late replication stage for differential staining, and R-banded chromosomes were obtained by exposing chromosome slides to UV light after staining with Hoechst 33258. DNA probes were labeled by nick translation with biotin-16-dUTP (Roche) using a standard protocol. Plasmids with insert cDNA longer than 0.7 kb were used as templates for labeling. The hybridized cDNA probes were reacted with goat anti-biotin antibodies (Vector Laboratories), and then stained with fluorescein-labeled donkey anti-goat IgG (Nordic Immunology). The slides were stained with 0.50 µg/ml propidium iodide for observation.

Gene mapping information for human, mouse and chicken chromosomes

Chromosomal locations of human and mouse genes were retrieved from NCBI Entrez Gene (URL: <http://www.ncbi.nih.gov/entrez/query.fcgi?db=gene>) and Ensembl. Mapping information of chicken genes was based on the previous studies (Suzuki *et al.* 1999; Guttenbach *et al.* 2000; Schmid *et al.* 2000) and Ensembl.

Results

*Identification of novel cDNAs in the Chinese soft-shelled turtle, *Pelodiscus sinensis**

With the reverse transcription-polymerase chain reaction (RT-PCR) using degenerate primers, we isolated and sequenced cDNA derived from 39 protein-coding genes

located in the nuclear genome of *P. sinensis* (Table 2). The total length of the sequenced cDNA fragments was 38,324 bp (9,527 amino acids). These sequences were deposited in GenBank under accession numbers AB188346-AB188384. Orthology to homologous genes reported in other vertebrates was rigorously confirmed for each gene by molecular phylogenetic trees constructed with the neighbor-joining method (Saitou & Nei 1987) and the maximum-likelihood method (Felsenstein 1981; Yang 1997). In these phylogenetic studies, we did not detect any gene duplications unique to the turtle lineage, indicating that the *P. sinensis* genome possesses a highly similar gene repertoire to that of other amniotes for these genes (data not shown).

Estimated number of synonymous substitutions between turtle and chicken

Including the sequences available in the public nucleotide sequence database GenBank (version 148.0), we selected 56 genes that satisfied the criteria that only a single ortholog should be found in *P. sinensis*, chicken, human and mouse, and that the orthologous sequences aligned between *P. sinensis* and chicken should be longer than 300 bp. For each pair, we estimated the number of synonymous (K_s) and non-synonymous substitution (K_a) between turtle and chicken (Table 3). The total length used for calculations was 26,268 bp (8,756 codons). The average K_s was 0.96 (standard deviation, 0.58; $n = 56$) under the maximum-likelihood method (Goldman & Yang 1994), and was 0.68 (standard deviation, 0.26; $n = 56$) under the method of Nei and Gojobori (1986). Positive selection ($K_a/K_s > 1$) was not detected in any of the 56 gene pairs (Table 3).

Distribution of GC₃ in turtle and other chordates

We calculated the GC₃ for 125 *P. sinensis* genes. In addition to the genes found in GenBank, we used cDNA sequences already deposited in the NCBI dbEST category (accession nos. AU312239-AU312301; Matsuda *et al.* 2005) with deduced protein-coding regions longer than 200 bp. The GC₃ of *P. sinensis* genes exhibited a bimodal distribution with an average of 55.7% and a standard deviation of 16.0% (Figure 2a), which was similar to that in chicken, human and sheep (*Ovis aries*) (standard deviation 16.3%-16.8%; Mann-Whitney U test, $P < 0.01$; Figures 2b, c). In contrast, non-amniotic vertebrates and invertebrates showed a unimodal distribution of GC₃ with a narrow standard deviation (7%-11%), although the averages varied extremely between species (40%-70%; Figures 2e-h). Mouse and rat also exhibited a unimodal distribution with averages of approximately 60%, and a much smaller standard deviation compared with the other amniotes (11%-12%; Figure 2d).

Cross-species GC₃ comparison between orthologs

To examine whether each turtle gene possessed a similar GC₃, we compared the GC₃ of the turtle genes with that of 56 genes from chicken (Figure 3a) and human (Figure 3b), for which we identified 1:1 ortholog pairs (Table 3). The turtle-chicken GC₃ comparison showed a significant positive correlation, with a correlation coefficient $r = 0.84$ (Spearman's rank correlation, $P < 0.001$), as did the turtle-human comparison with $r = 0.61$ ($P < 0.001$). Similarly, the human-chicken comparison exhibited a significant positive correlation with our gene set ($r = 0.63$, $P < 0.001$). In contrast, turtle-*Xenopus*

tropicalis and human-*X. tropicalis* comparisons of GC₃ for these 56 genes did not yield a significant correlation ($r = 0.09$ and $r = 0.11$, respectively) (Figures 3c, d).

Gene mapping on P. sinensis chromosomes

In this study, we treated chicken chromosomes 1-8, Z, and W, and the *P. sinensis* chromosomes 1-6 as macrochromosomes, and the rest of chromosomes as microchromosomes, following previous studies (McQueen *et al.* 1996; Matsuda *et al.* 2005; for karyotypic configuration of *P. sinensis* and chicken, see Discussion). We performed FISH mapping of 31 *P. sinensis* genes using cDNA clones isolated in this study as probes. Seventeen of the 31 genes were localized to the macrochromosomes, and the remaining 14 genes were localized to microchromosomes (Table 4). The five largest turtle chromosomes each corresponded to one chicken chromosome; chromosome numbers were equivalent between the turtle and chicken, with one exceptional case of the *PRRX1* gene (Table 4). The *FGF10* gene was localized to the turtle chromosome 6 (Table 4), which corresponded to the chicken sex Z chromosome (Matsuda *et al.* 2005). All the genes on the turtle chromosomes 7 and 8 were localized to the chicken chromosomes 7 and 6, respectively (Table 4). These results indicated that the eight largest turtle chromosomes each correspond to one chicken chromosome (chicken chromosomes 1–7 and chromosome Z), and confirmed that there is high level of conserved synteny along chromosomes between the turtle and chicken.

Comparison of GC₃ between macrochromosomes and microchromosomes of turtle and chicken

To corroborate the high GC-content in microchromosomes, previously shown by chromosome banding (Auer *et al.* 1987; Andreozzi *et al.* 2001) and whole genome sequencing (ICGSC 2004; also see Figure 4a), we compared the GC₃ between genes on macrochromosomes and microchromosomes, in chicken (Figure 4b) and *P. sinensis* (Figure 4c). We used 59 genes previously reported (Matsuda *et al.* 2005) and 31 genes mapped in this study (Table 4). The average GC₃ was 51.6% and 60.1% in chicken (Figure 4b), and 50.1% and 57.7% in *P. sinensis*, for macrochromosomes and microchromosomes, respectively. In *P. sinensis*, about 51.1% (23 out of 45 genes) of GC-rich genes (GC₃ ≥ 50%) resided on microchromosomes (47.9% in chicken) (Figure 5b), whereas 31.1% (14 out of 45 genes) of GC-poor genes (GC₃ < 50%) resided on microchromosomes (24.7% in chicken) (Figure 5c).

Discussion

Molecular phylogeny and evolutionary distance in sauropsids

Phylogenetic relationships between reptilian orders and birds have been controversial for decades (see Zardoya & Meyer 2001, for review). However, recent molecular phylogenetic analyses, using nuclear DNA-coded and mitochondrial DNA-coded genes, support a tree topology that places turtles closer to the Archosaurians (birds and crocodylians) than to the Lepidosaurians (tuataras, snakes, and lizards), in contrast to the archaic tree topology that positions turtles at a basal branch within the sauropsids

(Zardoya & Meyer 1998; Hedges & Poling 1999; Kumazawa & Nishida 1999; Cao *et al.* 2000; Rest *et al.* 2003; Iwabe *et al.* 2005).

In this study, we estimated the number of synonymous substitutions (K_s) in genes of the Chinese soft-shelled turtle, *P. sinensis*, and chicken, to measure the evolutionary distance between the two species at the molecular level, using 56 carefully chosen gene pairs that are conserved as a single ortholog in turtle, chicken, human and mouse (Table 3). The number of synonymous substitutions represents the amount of neutral substitutions accumulated in both lineages (Miyata & Yasunaga 1980) and, accordingly, serves as a standard index of the evolutionary distance between the two species. Our K_s estimation for the turtle-chicken gene pairs was 0.96 with the maximum-likelihood method (Goldman & Yang 1994), whereas previous studies using the same method have estimated the K_s for human-mouse gene pairs as 0.56 (RGSPC 2004) and for human-chicken gene pairs as 1.66 (ICGSC 2004). The difference between these figures is consistent with the above evolutionary hierarchy of amniote phylogeny, given that neutral substitution rates along these lineages have not dramatically changed. Additionally, it serves as a standard of evolutionary distance among these taxa and an indicator of orthology between genes in species belonging to these taxa.

GC₃ as a reflection of genomic GC level

In contrast to the homogeneous distribution of GC-content with sharp peaks in non-amniotic species, such as the tiger pufferfish (*Fugu rubripes*) and the tunicate (*Ciona intestinalis*) (Aparicio *et al.* 2002; Dehal *et al.* 2002), amniotes, such as human and chicken, show intra-genome GC heterogeneity; however, GC-content in rodent

genomes is somewhat homogeneous (Mouchiroud *et al.* 1988; MGSC 2002; RGSPC 2004) (Figure 1a). In this study, we focused on protein-coding regions rather than unavailable genomic sequences, because the GC₃ of a specific gene is expected to correlate with the global GC-content of the genomic region where the gene is found (Clay *et al.* 1996; Musto *et al.* 1999). Another advantage of focusing on protein-coding regions is that orthologies between corresponding chromosomal segments in different species are easily detectable with molecular phylogenetic analyses of genes harbored within these segments. In contrast, by focusing on protein-coding regions, we cannot incorporate the GC-content of non-coding DNA sequences, which make up a considerable proportion of a genome, into our present analysis. However, cross-species analysis of coding regions is an effective tool for focusing on orthologous genomic fractions derived from common ancestors by excluding the influence of the lineage-specific expansion of some specific genomic regions, such as repetitive elements. Another concern for imaginable pitfalls is that, in examining intra-genome GC heterogeneity, it is preferable to focus on a single species as a representative of the taxonomic group under investigation, because inter-species GC variation may mask the intra-genome GC landscape. For example, variable peaks of GC₃ distribution occur between the tiger pufferfish (*F. rubripes*) and the zebrafish (*Danio rerio*), which both belong to a single group of teleostei (Figure 2f).

Equivalence of the GC heterogeneity among amniotes

We isolated and sequenced 39 novel cDNAs from *P. sinensis*. Our subsequent GC₃ calculation for various chordates revealed that the GC₃ in *P. sinensis* exhibited a broad

and bimodal distribution, which had a strong resemblance to that in chicken and non-rodent mammals, such as human and sheep (Figures 2a-c), but not to that in non-amniotic species (Figures 2e-h) or rodents (Figure 2d). Similar results were obtained when GC-contents at four-fold degenerate sites (GC_4) were analyzed (data not shown).

The next question we addressed was whether the GC_3 distribution in turtle was derived from the common ancestor of mammals, reptiles and birds, or acquired secondarily in independent lineages. Thus, we performed a cross-species comparison of GC_3 between orthologs found in turtle, chicken and human. The results clearly showed that each turtle gene possesses a similar level of GC_3 to its ortholog in human and chicken, with statistically significant positive correlations (Figures 3a, b). The higher levels of GC_3 correlation between the turtle-chicken pair compared with the turtle-human pair can be explained by the lower levels of neutral substitutions and translocations that accumulated in the turtle-chicken pair, which may have caused a secondary decay of ancestral intra-genome GC-bias. Our ortholog set also exhibited a significant positive correlation between GC_3 and GC-content of the surrounding genomic region (10 kb on each side) in chicken (Spearman's $r = 0.65$, $P < 0.005$) (Figure 6). To rule out the possibility that the limited number of genes has yielded misleading results because of a biased choice of genes, we then confirmed that the GC_3 distribution in the set of orthologous genes examined significantly resembled that obtained with an original large set of cDNAs in human and chicken, respectively (Mann-Whitney U test, $P < 0.01$ for both; data not shown). Despite that our gene set is limited in number, it seems sufficient to speculate the overall features of the turtle genome. In conclusion, taking into account the results of the present analysis with 56

orthologous genes, along with previous observations that GC₃ levels have been highly conserved in a large set of orthologous genes between human and chicken (Kadi *et al.* 1993; Bernardi 2000), the most parsimonious interpretation is that orthologous genomic regions in these three species have maintained similar GC-contents which were derived from the last common ancestor of mammals, birds, and reptiles.

In contrast, we detected no significant correlation in a comparison of GC₃ between turtle and *X. tropicalis* for the above ortholog pairs (Figures 3c, d); however, Bernardi (2000) have reported a weak positive correlation in GC₃ between human and *X. laevis*. At present, whether the origin of intra-genome GC heterogeneity antedated the common ancestors of amniotes and amphibians remains unanswered.

Differences in gene density between macrochromosomes and microchromosomes

The diploid chromosome number of *P. sinensis* is $2n = 66$, which consists of six pairs of macrochromosomes and 27 pairs of microchromosomes (Matsuda *et al.* 2005), whereas the chicken karyotype ($2n = 78$) consists of nine pairs of macrochromosomes, including the ZW sex chromosomes, and 29 pairs of microchromosomes. In chicken, it was suggested that microchromosomes contain up to 50% of the genes in the genome and represent about 23% of total genomic DNA, indicating that the gene density on microchromosomes is two to three times higher than that on macrochromosomes (Smith *et al.* 2000). In this study, we found that 41.1% (37 out of 90 genes) of turtle genes localize to microchromosomes (Figure 5a). This figure resembles that observed in chicken (37.4%; 3132 out of 8380 genes; Figure 5a). Although this trend is now roughly confirmed with genomic sequences only in chicken (ICGSC 2004), further efforts will

be required to unveil a gene distribution on turtle chromosomes. Additionally, the genes we used represent all the macrochromosomes and some microchromosomes in chicken and *P. sinensis* (Table 4), which suggests these genes serve as random markers for whole genomic regions.

Difference in GC-content between macrochromosomes and microchromosomes

Unlike in mammals, the average intra-chromosomal GC-content in chicken increases with the reduction in chromosomal length (Figure 1b). In this context, our gene mapping detected a difference in GC₃ distribution between macrochromosomes and microchromosomes (Figure 4). In *P. sinensis* and chicken, GC-poor genes are two to three times more likely to reside on macrochromosomes than on microchromosomes (Figure 5c), whereas GC-rich genes tend to reside equally on macrochromosomes and microchromosomes (Figure 5b). Thus, macrochromosomes tend to contain more GC-poor genes (Figure 5d), whereas microchromosomes tend to contain more GC-rich genes (Figure 5e). In contrast, there is no significant correlation between GC₃ and the size of chromosomes harboring them in human and mouse (data not shown), which is consistent with the analysis at the genomic level (Figures 1b-e). Accordingly, chromosomal size-dependent GC compartmentalization seems to be unique to sauropsids whose karyotypes consist of macrochromosomes and microchromosomes.

Insight into the evolutionary history of intra-genome GC heterogeneity

We conclude that the base composition in the turtle genome has a strong resemblance to

its chicken counterpart; that is, the turtle genome exhibits a high level of intra-genome GC heterogeneity, and a higher proportion of GC-rich genes on microchromosomes (Figure 5e). This conclusion is incompatible with previous observations using chromosome banding studies (Holmquist 1989) and density gradient centrifugation (Thiery *et al.* 1976; Hughes *et al.* 2002), which reported the lower level of GC heterogeneity in the turtle genome. Apart from the problems in sensitivity of the above indirect methods, the effect of lineage-specific events such as expansion of repetitive elements with extreme GC-contents might reconcile this difference. After all, to understand the evolutionary history of intra-genome GC bias, studies focusing on protein-coding regions might be more likely to detect features derived from the common ancestors.

The intra-genome distribution of GC-rich and GC-poor regions has not been clarified in other sauropsids. However, the karyotype of the common ancestor of extant sauropsids is thought to have contained both macrochromosomes and microchromosomes (Burt 2002; Norris *et al.* 2004), although some lineages underwent frequent secondary fusion of microchromosomes resulting in no or few microchromosomes as seen in the reptilian family Crocodylidae and the avian family Falconiformes (Cohen & Gans 1970; De Boer & Sinoo 1984). In contrast, chromosome sizes are relatively uniform and there is no striking bias in inter-chromosomal GC-content in most mammals. These facts indicate that sauropsids adopted a chromosomal size-dependent GC compartmentalization strata, whereas mammals maintained the system in which GC-rich and GC-poor regions coexist on individual chromosomes in a highly juxtaposed manner (Figure 7). This hypothesis has yet to be verified by further large-scale studies, not only in turtle, but also in other sauropsids.

Furthermore, it is important to clarify whether monotremes, marsupials and amphibians have a similar pattern of intra-genome GC distribution to eutherians, in order to speculate on the ancestral configuration for the amniote genome by adding outgroup polarity to the present scheme.

The genomic landscape of base composition cannot be comprehensively realized without elaborate genomic sequencing. However, our approaches of cDNA sequencing followed by cDNA-based gene mapping and *in silico* GC₃ calculation have revealed a shared GC heterogeneity of the Chinese soft-shelled turtle *P. sinensis* and chicken. In this study, as a source of material in GC profiling in the turtle, we cloned and sequenced cDNAs of limited number of protein-coding genes, especially because we observed in our preliminary studies that a high-throughput sequencing of cDNAs, such as expression sequence tags (ESTs), did not always reproduce GC distribution of whole gene repertoires in chicken and human, possibly due to some experimental biases or correlation between GC level of genes and their expression levels. Therefore, we carefully examined in chicken and human whether our gene set reproduces GC distribution of whole genes and even of whole genomes. As long as such attention is paid, our approach serves as an informative tool for surveying genomic features in non-model organisms for which there is a limited amount of genomic sequence information.

Acknowledgements

We are very grateful to Ryo Usuda for technical assistance in cDNA cloning and

sequencing, and to Kanako O. Koyanagi and Kazutaka Katoh for valuable comments and discussion. This work was supported by Grants-in-Aid for Scientific Research from the Ministry of Education, Culture, Sports, Science and Technology in Japan and the Grant for Biodiversity Research of the 21st Century COE (A14).

References

- Altschul SF, Madden TL, Schaffer AA *et al.* (1997) Gapped BLAST and PSI-BLAST: a new generation of protein database search programs. *Nucleic Acids Res* **25**: 3389-3402.
- Andreozzi L, Federico C, Motta S *et al.* (2001) Compositional mapping of chicken chromosomes and identification of the gene-richest regions. *Chromosome Res* **9**: 521-532.
- Aparicio S, Chapman J, Stupka E *et al.* (2002) Whole-genome shotgun assembly and analysis of the genome of *Fugu rubripes*. *Science* **297**: 1301-1310.
- Auer H, Mayr B, Lambrou M, Schleger W (1987) An extended chicken karyotype, including the NOR chromosome. *Cytogenet Cell Genet* **45**: 218-221.
- Belle EM, Smith N, Eyre-Walker A (2002) Analysis of the phylogenetic distribution of isochores in vertebrates and a test of the thermal stability hypothesis. *J Mol Evol* **55**: 356-363.
- Bernardi G (2000) Isochores and the evolutionary genomics of vertebrates. *Gene* **241**: 3-17.
- Bernardi G, Olofsson B, Filipinski J *et al.* (1985) The mosaic genome of warm-blooded vertebrates. *Science* **228**: 953-958.
- Burt DW (2002) Origin and evolution of avian microchromosomes. *Cytogenet Genome Res* **96**: 97-112.
- Cao Y, Sorenson MD, Kumazawa Y, Mindell DP, Hasegawa M (2000) Phylogenetic position of turtles among amniotes: evidence from mitochondrial and nuclear genes. *Gene* **259**: 139-148.

- Clay O, Caccio S, Zoubak S, Mouchiroud D, Bernardi G (1996) Human coding and noncoding DNA: compositional correlations. *Mol Phylogenet Evol* **5**: 2-12.
- Cohen MM, Gans C (1970) The chromosomes of the order Crocodylia. *Cytogenetics* **9**: 81-105.
- De Boer LEM, Sinoo RP (1984) A karyological study of Accipitridae (Aves: Falconiformes), with karyotypic description of 16 species new to cytology. *Genetica* **65**: 89-107.
- Dehal P, Satou Y, Campbell RK *et al.* (2002) The draft genome of *Ciona intestinalis*: insights into chordate and vertebrate origins. *Science* **298**: 2157-2167.
- Eyre-Walker A, Hurst LD 2001. The evolution of isochores. *Nat Rev Genet* **2**: 549-555.
- Felsenstein, J (1981) Evolutionary trees from DNA sequences: a maximum likelihood approach. *J Mol Evol* **17**: 368-376.
- Frohman MA, Dush MK, Martin GR (1988) Rapid production of full-length cDNAs from rare transcripts: amplification using a single gene-specific oligonucleotide primer. *Proc Natl Acad Sci USA* **85**: 8998-9002.
- Goldman, N, Yang, Z (1994) A codon-based model of nucleotide substitution for protein-coding DNA sequences. *Mol Biol Evol* **11**: 725-736.
- Graves, JA, Westerman, M (2002) Marsupial genetics and genomics. *Trends Genet* **18**: 517-521.
- Grützner F, Deakin J, Rens W, El-Mogharbel N, Marshall Graves JA (2003) The monotreme genome: a patchwork of reptile, mammal and unique features? *Comp Biochem Physiol A Mol Integr Physiol* **136**: 867-881.
- Guttenbach M, Nanda I, Brickell PM *et al.* (2000) Chromosomal localization of the genes encoding ALDH, BMP-2, R-FABP, IFN-gamma, RXR-gamma, and VIM

- in chicken by fluorescence in situ hybridization. *Cytogenet Cell Genet* **88**: 266-271.
- Hamada K, Horiike T, Ota H, Mizuno K, Shinozawa T (2003) Presence of isochore structures in reptile genomes suggested by the relationship between GC contents of intron regions and those of coding regions. *Genes Genet Syst* **78**: 195-198.
- Hedges SB, Poling LL (1999) A molecular phylogeny of reptiles. *Science* **283**: 998-1001.
- Holmquist GP (1989) Evolution of chromosome bands: molecular ecology of noncoding DNA. *J Mol Evol* **28**: 469-486.
- Hubbard T, Andrews D, Caccamo M *et al.* (2005) Ensembl 2005. *Nucleic Acids Res* **33**: D447-453.
- Hughes S, Clay O, Bernardi G (2002) Compositional patterns in reptilian genomes. *Gene* **295**: 323-329.
- Hughes S, Zelus D, Mouchiroud D (1999) Warm-blooded isochore structure in Nile crocodile and turtle. *Mol Biol Evol* **16**: 1521-1527.
- International Chicken Genome Sequencing Consortium (ICGSC) (2004) Sequence and comparative analysis of the chicken genome provide unique perspectives on vertebrate evolution. *Nature* **432**: 695-716.
- International Human Genome Sequence Consortium (IHGSC) (2001) Initial sequencing and analysis of the human genome. *Nature* **409**: 860-921.
- Iwabe N, Hara Y, Kumazawa Y *et al.* (2005) Sister group relationship of turtles to the bird-crocodylian clade revealed by nuclear DNA-coded proteins. *Mol Biol Evol* **22**: 810-813.
- Jaillon O, Aury JM, Brunet F *et al.* (2004) Genome duplication in the teleost fish

- Tetraodon nigroviridis* reveals the early vertebrate proto-karyotype. *Nature* **431**: 946-957.
- Kadi F, Mouchiroud D, Sabeur G, Bernardi G (1993) The compositional patterns of the avian genomes and their evolutionary implications. *J Mol Evol* **37**: 544-551.
- Katoh K, Misawa K, Kuma K, Miyata T (2002) MAFFT: a novel method for rapid multiple sequence alignment based on fast Fourier transform. *Nucleic Acids Res* **30**: 3059-3066.
- Kumazawa Y, Nishida M (1999) Complete mitochondrial DNA sequences of the green turtle and blue-tailed mole skink: statistical evidence for archosaurian affinity of turtles. *Mol Biol Evol* **16**: 784-792.
- Matsuda Y, Chapman VM (1995) Application of fluorescence in situ hybridization in genome analysis of the mouse. *Electrophoresis* **16**: 261-272.
- Matsuda Y, Nishida-Umehara C, Tarui H *et al.* (2005) Highly conserved linkage homology between birds and turtles: Bird and turtle chromosomes are precise counterparts of each other. *Chromosome Res* **13**: 601-615.
- McQueen HA, Fantes J, Cross SH, Clark VH, Archibald AL, Bird AP (1996) CpG islands of chicken are concentrated on microchromosomes. *Nat Genet* **12**: 321-324.
- McQueen HA, Siriaco G, Bird AP (1998) Chicken microchromosomes are hyperacetylated, early replicating, and gene rich. *Genome Res* **8**: 621-630.
- Mouse Genome Sequencing Consortium (MGSC) (2002) Initial sequencing and comparative analysis of the mouse genome. *Nature* **420**: 520-562.
- Miyata T, Yasunaga T (1980) Molecular evolution of mRNA: a method for estimating evolutionary rates of synonymous and amino acid substitutions from

- homologous nucleotide sequences and its application. *J Mol Evol* **16**: 23-36.
- Mouchiroud D, Gautier C, Bernardi G (1988) The compositional distribution of coding sequences and DNA molecules in humans and murids. *J Mol Evol* **27**: 311-320.
- Musto H, Romero H, Zavala A, Bernardi G (1999) Compositional correlations in the chicken genome. *J Mol Evol* **49**: 325-329.
- Nei M, Gojobori T (1986) Simple methods for estimating the numbers of synonymous and nonsynonymous nucleotide substitutions. *Mol Biol Evol* **3**: 418-426.
- Norris TB, Rickards GK, Daugherty CH (2004) Chromosomes of tuatara, *Sphenodon*, a chromosome heteromorphism and an archaic reptilian karyotype. *Cytogenet Genome Res* **105**: 93-99.
- Phillips MJ, Penny D (2003) The root of the mammalian tree inferred from whole mitochondrial genomes. *Mol Phylogenet Evol* **28**: 171-185.
- Rest JS, Ast JC, Austin CC *et al.* (2003) Molecular systematics of primary reptilian lineages and the tuatara mitochondrial genome. *Mol Phylogenet Evol* **29**: 289-297.
- Rat Genome Sequencing Project Consortium (RGSP) (2004) Genome sequence of the Brown Norway rat yields insights into mammalian evolution. *Nature* **428**: 493-521.
- Saitou N, Nei M (1987) The neighbor-joining method: a new method for reconstructing phylogenetic trees. *Mol Biol Evol* **4**: 406-425.
- Schmid M, Nanda I, Guttenbach M *et al.* (2000) First report on chicken genes and chromosomes 2000. *Cytogenet Cell Genet* **90**: 169-218.
- Smith J, Bruley CK, Paton IR *et al.* (2000) Differences in gene density on chicken macrochromosomes and microchromosomes. *Anim Genet* **31**: 96-103.

- Stajich JE, Block D, Boulez K *et al.* (2002) The Bioperl toolkit: Perl modules for the life sciences. *Genome Res* **12**: 1611-1618.
- Suzuki T, Kurosaki T, Shimada K *et al.* (1999) Cytogenetic mapping of 31 functional genes on chicken chromosomes by direct R-banding FISH. *Cytogenet Cell Genet* **87**: 32-40.
- Thiery JP, Macaya G, Bernardi G (1976) An analysis of eukaryotic genomes by density gradient centrifugation. *J Mol Biol* **108**: 219-235.
- Yang Z (1997) PAML: a program package for phylogenetic analysis by maximum likelihood. *Comput Appl Biosci* **13**: 555-556.
- Zardoya R, Meyer A (1998) Complete mitochondrial genome suggests diapsid affinities of turtles. *Proc Natl Acad Sci USA* **95**: 14226-14231.
- Zardoya R, Meyer A (2001) The evolutionary position of turtles revised. *Naturwissenschaften* **88**: 193-200.

Figure legends

Figure 1. Overview of intra-genome GC-content in chordates revealed by whole genome sequencing. **(a)** Distribution of GC-content in non-overlapping 20 kb windows for human (blue), mouse (yellow), chicken (red), tiger pufferfish (*Fugu rubripes*) (green), and tunicate (*Ciona intestinalis*) (grey). For simplicity, we excluded data for rat in which intra-genome GC heterogeneity highly resembles that of mouse (RGSPC 2004). **(b-e)** Chromosomal length and global GC-content. Overall GC-content (%) and chromosome length are plotted for chicken **(b)**, human **(c)**, mouse **(d)**, and green pufferfish (*Tetraodon nigroviridis*; Jaillon *et al.* 2004) **(e)**. Chromosomal GC-content was calculated as the proportion of guanine or cytosine within the length of nucleotide sequence that had already been determined. Chromosomes with less than 70% sequencing coverage were excluded from the analysis. Note that the horizontal axes are not to equal scale. Genomic sequences sorted by chromosomes and estimated chromosome lengths were retrieved from Ensembl.

Figure 2. Distribution of GC-content in exonic third positions (GC₃) in various chordates. Distribution of GC₃ are shown as histograms for genes of the Chinese soft-shelled turtle (*P. sinensis*) (n = 125) **(a)**; chicken (n = 8380) **(b)**; human (n = 23636) and sheep (*Ovis aries*) (n = 1436) **(c)**; mouse (n = 22376) and rat (n = 21009) **(d)**; *Xenopus tropicalis* (n = 1815) and axolotl (*Ambystoma mexicanum*) (n = 4257) **(e)**; zebrafish (*Danio rerio*) (n = 3653) and tiger pufferfish (*Fugu rubripes*) (n = 23285) **(f)**; amphioxus (*Branchiostoma belcheri*) (n = 199) and tunicate (*Ciona intestinalis*) (n = 12588) **(g)**; and *Drosophila melanogaster* (n = 12862) and *Caenorhabditis elegans* (n =

16341) **(h)**.

Figure 3. Cross-species comparison of GC₃ between orthologs. Two-dimensional plots of GC₃ for 56 ortholog pairs are shown for turtle-chicken **(a)** and turtle-human **(b)**. Two-dimensional plots of GC₃ comparison for *P. sinensis* and *Xenopus tropicalis* **(c)** and human and *X. tropicalis* **(d)** are also shown for 41 genes whose *X. tropicalis* orthologs were found in the Ensembl (URL: <http://www.ensembl.org/>).

Figure 4. Distribution of GC-content on macrochromosomes and microchromosomes. Distribution of global GC-content of genomic sequences on macrochromosomes and microchromosomes of chicken is shown as a histogram in 20 kb non-overlapping windows **(a)**; distribution of GC-content in exonic third positions (GC₃) for 90 *P. sinensis* genes **(b)**; and distribution of GC₃ for 8380 chicken cDNAs **(c)**.

Figure 5. GC-content of turtle and chicken genes in relation to their location on macrochromosomes and microchromosomes. Circle graphs representing the relative proportion of genes located on macrochromosomes and microchromosomes are shown for all genes analyzed **(a)**; GC-rich genes (GC₃ ≥ 50%) **(b)**; and GC-poor genes (GC₃ < 50%) **(c)**. Relative proportions of GC-rich and GC-poor genes out of those located on macrochromosomes **(d)** and microchromosomes **(e)** are also shown.

Figure 6. Correlation of GC-content in exonic third positions (GC₃) and surrounding genomic regions in chicken. Two-dimensional plots of GC₃ for chicken cDNAs and GC-contents of the genomic regions (10 kb on each side) in which the gene is located

are shown for 53 genes whose flanking genomic sequences were found in the Ensembl Chicken Genome Server (URL: http://www.ensembl.org/Gallus_gallus/), out of 56 genes used in this study.

Figure 7. Schematic representation of chromosomal evolution and transition of base composition in amniote phylogeny. Hypothesized evolutionary model for macrochromosome and microchromosome karyotypic configuration and intra-genome GC heterogeneity is illustrated in accordance with phylogenetic relationships revealed by recent molecular phylogenetic analyses (Phillips & Penny 2003; Rest *et al.* 2003; Iwabe *et al.* 2005). The intensity of monochrome tone in the chromosome image represents the relative extent of intra-chromosomal GC-content. Lepidosaurians tend to have microchromosomes (Norris *et al.* 2004) as do most other sauropsids; however, their GC profiles have not yet been obtained. Marsupials possess only large chromosomes (Graves & Westerman 2002), and thus are expected to show a eutherian mode of intra-genome base composition. Karyotypes of monotremes are denoted as a ‘patchwork’ of other mammals and reptiles because of the co-existence of large and small chromosomes (Grützner *et al.* 2003). However, there are no reports on GC profiles in these non-eutherian mammals. See text for details about rodents and crocodiles.

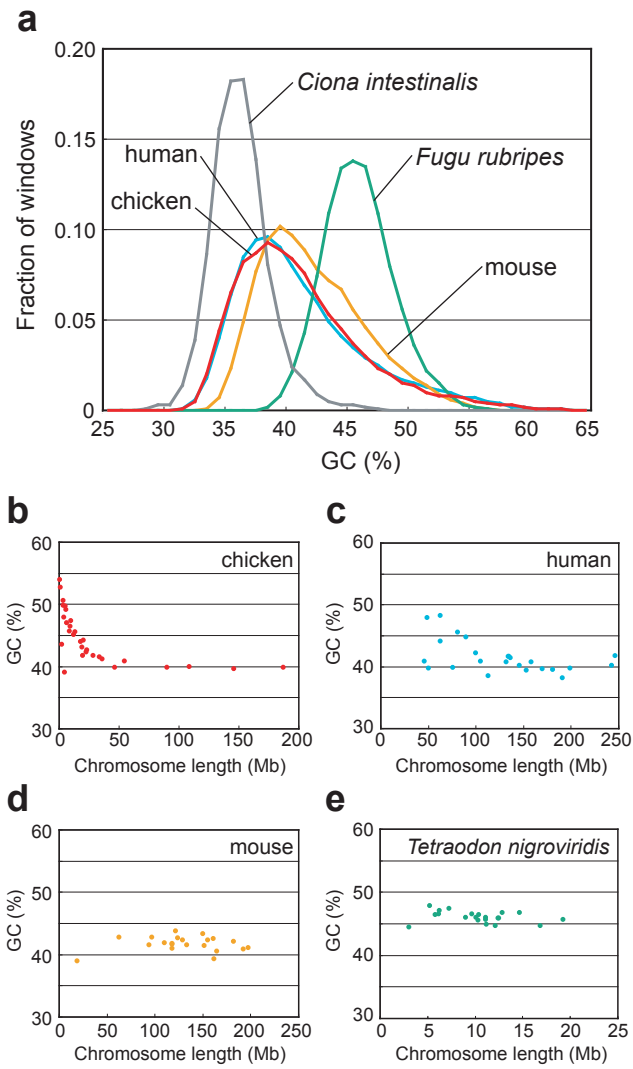


Figure 1

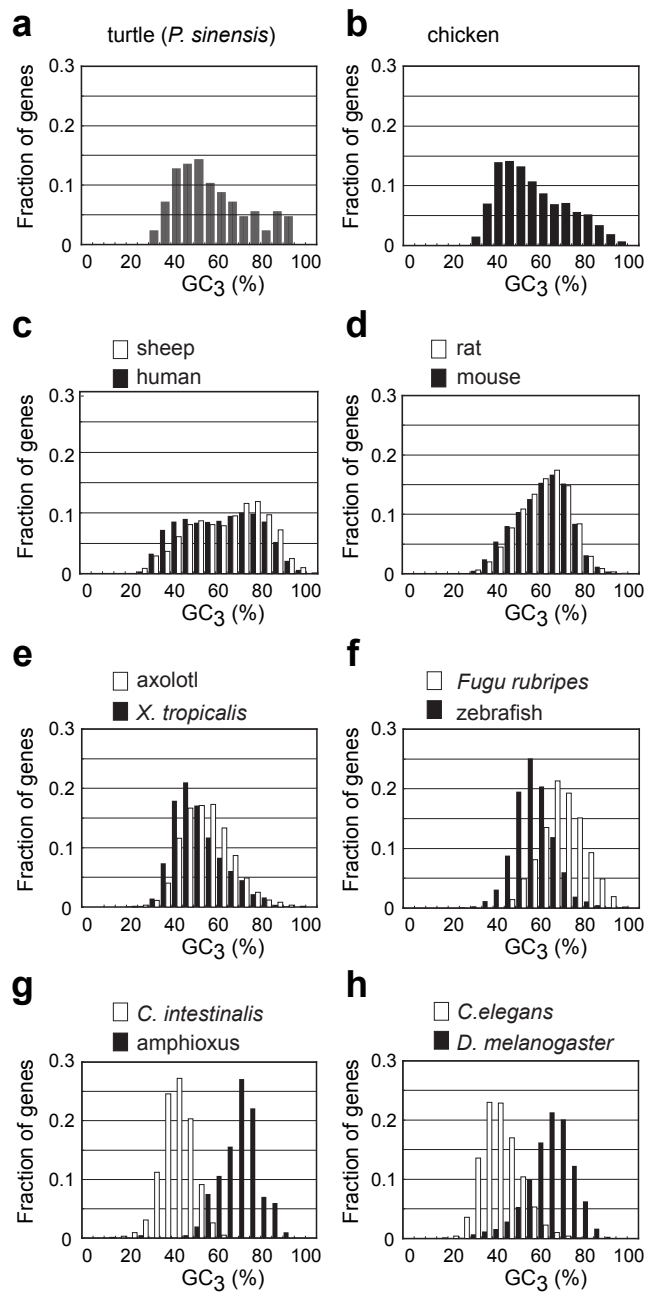


Figure 2

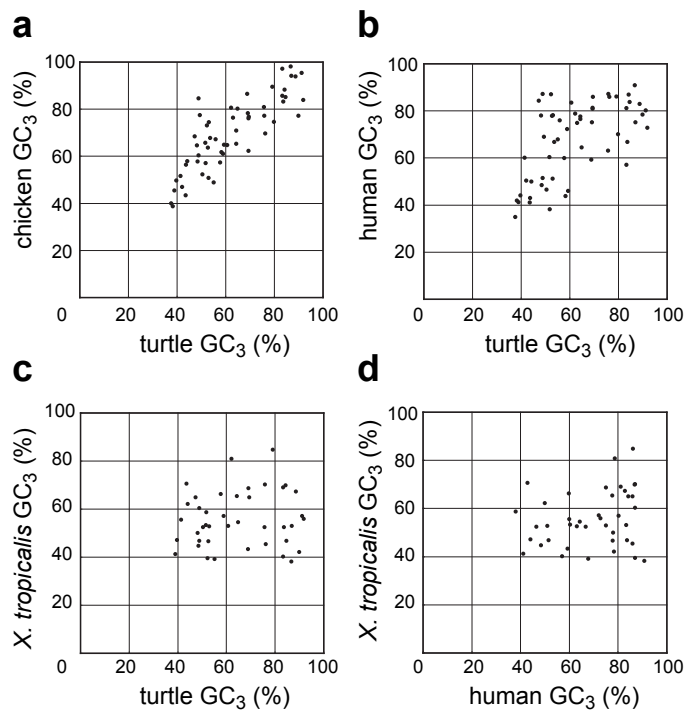


Figure 3

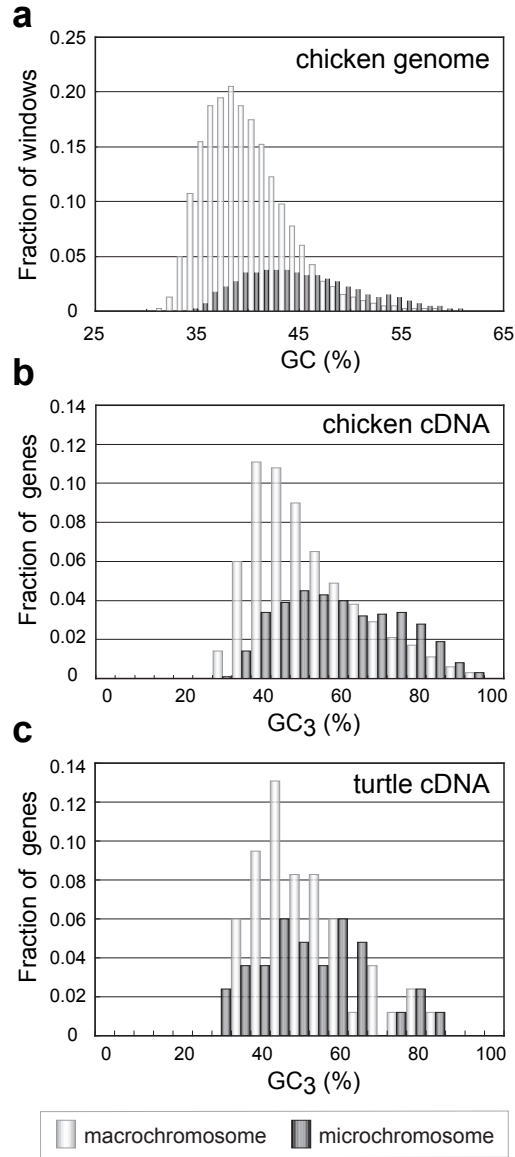


Figure 4

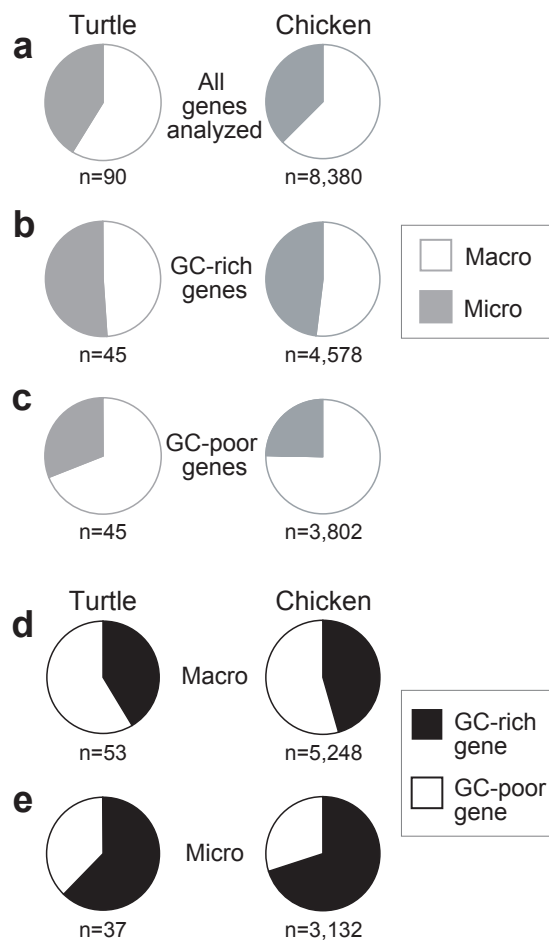


Figure 5

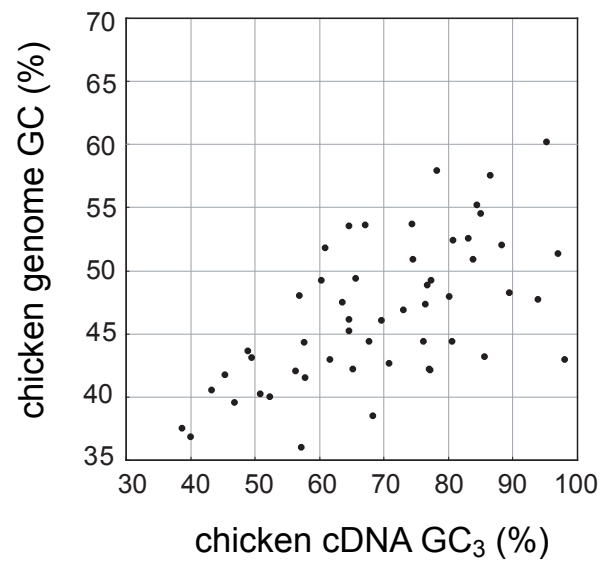


Figure 6

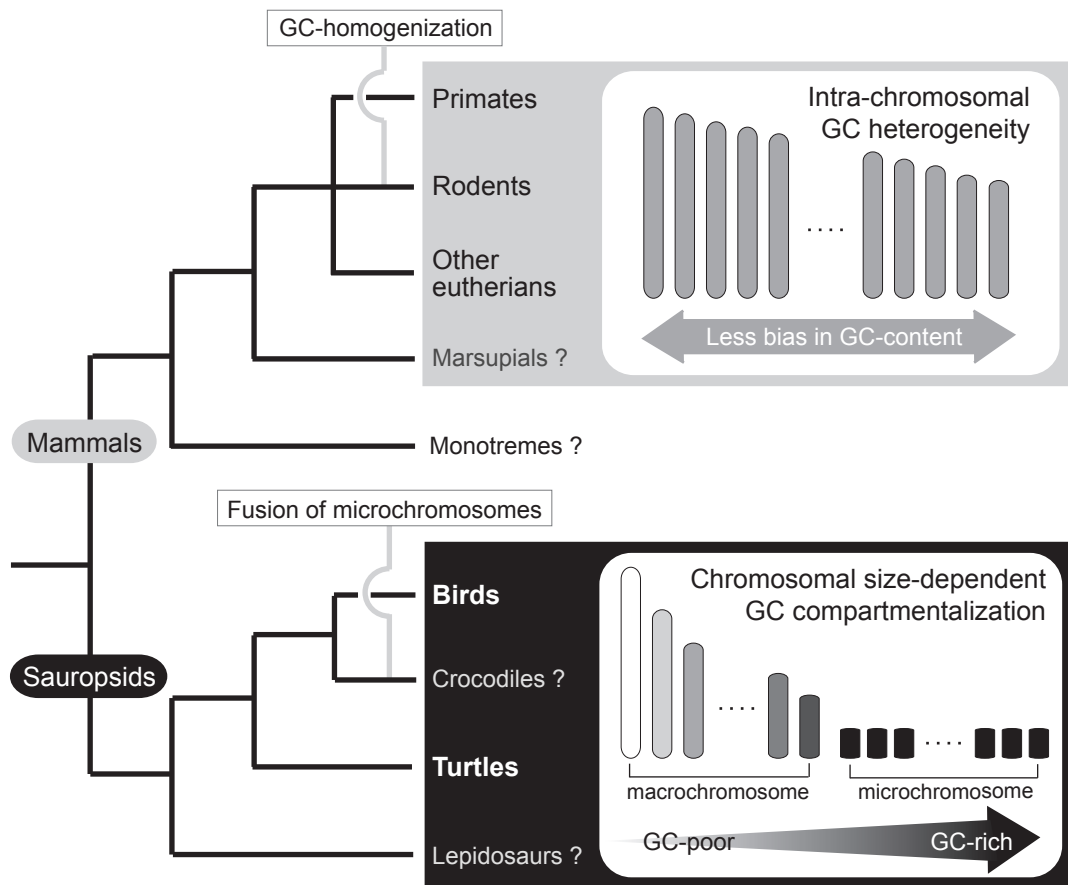


Figure 7

Table 1. Degenerate oligonucleotide primers used for isolation of unidentified cDNAs

| Gene ^a | Forward primer (5'-3') | Reverse primer (5'-3') |
|------------------------------------|-------------------------------|-----------------------------|
| <i>HOXD13</i> | CACTTCGGSAAYGGNTAYTAYWSNTG | CGCTTCATNCKNCKRTTYTGRAACCA |
| <i>PRRX1</i> (Prx1) | GCGCAAGCTMGNAARAAYTTYWSNGT | CGGTTCCGDATNSWRTTNGCCATRTT |
| <i>EN1</i> | TGGCCAGCNTGGGTNTAYTGYACNMG | GTGCTGTGGTTRTANARNCCYTGNCG |
| <i>EMX2</i> | TACACGAAYCCNGAYTNGTNTTYGC | GGRAACCANACYTTNACYTGNNGTYTC |
| <i>PAX3</i> | GAARATHGTNGARATGGCNCAICYG | CCGGGDATNARRTGRTRRAANGCCAT |
| <i>PAX7</i> | GAARATHGTNGARATGGCNCAICYG | CCTGGTAANARRTGRTRRAANGCNGC |
| <i>TCF7L2</i> (TCF4) | GGAAAYGCNTTYATGYTNTAYATGAARGA | TTACCATAGTTRTCNCKNGCNSWCCA |
| <i>RARA/RARG</i> ^b | GAACAAGGTAACNMGNAAYMGNTGYCA | CCWGCRTTRTGCATYTGNGTNCCKRTT |
| <i>RARB</i> | CGCGTNTAYAARCCNTGYTTYGTNTG | GTCAARTCRTCNARYTCNGCNGTCA |
| <i>MYOD1</i> (MyoD) | GGGCTTGAYAARGCNTGYAARMGNAAR | GCGTTCCTAARDATNTCNACYTTNGG |
| <i>GLI2</i> | GAGAARAARGARTTYGTNTGYMGNTGG | TCGAGATAGGRTCRTANSWRTCNGC |
| <i>GLI3</i> | GAGAARAARGARTTYGTNTGYMGNTGG | GACCRGNACNGTYTTNACRTGYTT |
| <i>SHH/IHH/DHH</i> ^b | TNACNGARGGNTGGGAYGARGAYG | TAGTRNACCCARTCRAANCCNGCYTC |
| <i>WNT2B/4/11</i> ^b | TAAATGTCACGGAGTAWSNNGNWSNTG | GACNNARCACCARTGRAAYTTRCA |
| <i>WNT3A</i> | GGNATHCARGARTGYCAYCARCAYTT | CCACAACATAGNARNNTYRCANCCRTC |
| <i>WNT5A</i> | GGTGCNAARACNGGNATHAARGARTG | GACNNARCACCARTGRAAYTTRCA |
| <i>WNT7A</i> | TAGGAGAGMGNACNGTNTTYGGNA | GCGCWRANGTRTRCAYTTNACRTA |
| <i>WNT8A</i> | TTCCTGATWACNGGNCNAARGCNTA | GACNNARCACCARTGRAAYTTRCA |
| <i>BMP2/4/7</i> ^b | GTGCCGCCNTAYATGYTNGAYYTNTA | TCDATCCARTCRTTCCANCCNACRTC |
| <i>LFNG/RFNG/MFNG</i> ^b | GACGTGTTYATHGCNGTNAARACNAC | TGCAGGTTCTCNARRTGNWSRTGRAA |
| <i>FGFR1/2/4</i> ^b | CCTTTWGGNGARGGNTGYTTYGGNCA | GAGCCNCCNARNGTAAADATYTCCCA |
| <i>CDH1</i> (E-cadherin) | TACGNGAYTGGGTNATHCCNCCNAT | GATGAARTNCCDATYTCRTCNGGRTT |
| <i>TWIST2</i> (dermo-1) | CAGGTGYTNCARWSNGAYGARATG | CACCTTCATNCKCCANACNSWRAA |
| <i>FOXA1</i> (HNF3 α) | GAGCNGTNAARATGGARGGNCAICY | GGTARCANCCRTTYTCRAACATRTTNC |

^aGene names were indicated as gene symbols designated for human orthologs. Famous aliases for gene names are also added in parenthesis. ^bA single set of degenerate primers were used for amplification of multiple phylogenetically close paralogs. Degenerative nucleotides are shown following IUB code.

Table 2. List for cDNAs newly isolated from *P. sinensis* in this study.

| Gene symbol ^a | Gene name | Accession Number |
|--------------------------|---|------------------|
| <i>HOXD13</i> | homeobox D13 | AB188346 |
| <i>PRRX1</i> | paired related homeobox 1 | AB188347 |
| <i>EN1</i> | engrailed homolog 1 | AB188348 |
| <i>EMX2</i> | empty spiracles homolog 2 | AB188349 |
| <i>PAX3</i> | paired box gene 3 | AB188350 |
| <i>PAX7</i> | paired box gene 7 | AB188351 |
| <i>TCF7L2</i> | transcription factor 7-like2 (T-cell factor 4) | AB188352 |
| <i>RARA</i> | retinoic acid receptor, alpha | AB188353 |
| <i>RARB</i> | retinoic acid receptor, beta | AB188354 |
| <i>RARG</i> | retinoic acid receptor, gamma | AB188355 |
| <i>MYOD1</i> | myogenic factor 3 (myoD) | AB188356 |
| <i>GLI2</i> | GLI-Kruppel family member GLI2 | AB188357 |
| <i>GLI3</i> | GLI-Kruppel family member GLI3 | AB188358 |
| <i>IHH</i> | Indian hedgehog | AB188359 |
| <i>WNT2B</i> | wingless-type MMTV integration site family, member 2B | AB188360 |
| <i>WNT3A</i> | wingless-type MMTV integration site family, member 3A | AB188361 |
| <i>WNT4</i> | wingless-type MMTV integration site family, member 4 | AB188362 |
| <i>WNT5A</i> | wingless-type MMTV integration site family, member 5A | AB188363 |
| <i>WNT7A</i> | wingless-type MMTV integration site family, member 7A | AB188364 |
| <i>WNT8A</i> | wingless-type MMTV integration site family, member 8A | AB188365 |
| <i>WNT11</i> | wingless-type MMTV integration site family, member 11 | AB188366 |
| <i>BMP7</i> | bone morphogenetic protein 7 | AB188367 |
| <i>LFNG</i> | lunatic fringe homolog | AB188368 |
| <i>RFNG</i> | radical fringe homolog | AB188369 |
| <i>MFNG</i> | manic fringe homolog | AB188370 |
| <i>FGFR1</i> | fibroblast growth factor receptor 1 | AB188371 |
| <i>FGFR2</i> | fibroblast growth factor receptor 2 | AB188372 |
| <i>FGFR4</i> | fibroblast growth factor receptor 4 | AB188373 |
| <i>CDH1</i> | cadherin 1, type 1 (E-cadherin) | AB188374 |
| <i>THOC2</i> | THO complex 2 | AB188375 |
| <i>RPL23</i> | ribosomal protein L23 | AB188376 |
| <i>RPS20</i> | ribosomal protein S20 | AB188377 |
| <i>RPL30</i> | ribosomal protein L30 | AB188378 |
| <i>TWIST2</i> | twist-related dermis-expressed protein 1 (Dermo-1) | AB188379 |
| <i>SKI</i> | v-ski sarcoma viral oncogene homolog (c-ski) | AB188380 |
| <i>TCF7L1</i> | transcription factor 7-like 1 (TCF3) | AB188381 |
| <i>FOXA1</i> | forkhead box A1 (HNF3alpha) | AB188382 |
| <i>DHH</i> | desert hedgehog | AB188383 |
| <i>DDX46</i> | DEAD box polypeptide 46 (Prp5-like) | AB188384 |

^aGene names were indicated as gene symbols designated for human orthologs.

Table 3. Estimated number of synonymous and non-synonymous substitutions in orthologous gene pairs of turtle and chicken.

| Gene symbol ^a | Accession number for <i>P. sinensis</i> | Aligned length (nt) | ML | | Nei-Gojobori ^d | |
|--------------------------|--|------------------------|-----------|-----------|---------------------------|-----------|
| | | | <i>Ka</i> | <i>Ks</i> | <i>Ka</i> | <i>Ks</i> |
| <i>HOXD13</i> | AB188346 ^b | 615 | 0.02 | 0.92 | 0.02 | 0.78 |
| <i>MSX1</i> | AB124572 | 735 ^c | 0.04 | 1.01 | 0.05 | 0.54 |
| <i>MSX2</i> | AB181139 | 594 | 0.02 | 0.60 | 0.02 | 0.53 |
| <i>PRRX1</i> | AB188347 ^b | 540 | 0.02 | 1.17 | 0.02 | 0.79 |
| <i>EN1</i> | AB188348 ^b | 312 | 0.01 | 2.65 | 0.02 | 0.61 |
| <i>EMX2</i> | AB188349 ^b | 540 | 0.01 | 0.53 | 0.01 | 0.54 |
| <i>PAX3</i> | AB188350 ^b | 1254 | 0.01 | 0.55 | 0.01 | 0.59 |
| <i>PAX7</i> | AB188351 ^b | 1308 | 0.01 | 0.82 | 0.01 | 0.68 |
| <i>PAX9</i> | AB181136 | 714 | 0.11 | 1.29 | 0.12 | 0.98 |
| <i>LEF1</i> | AB124566 | 1107 ^c | 0.02 | 0.47 | 0.02 | 0.55 |
| <i>TCF7L2</i> | AB188352 ^b | 303 | 0.00 | 0.19 | 0.00 | 0.21 |
| <i>RARA</i> | AB188353 ^b | 804 | 0.01 | 1.83 | 0.02 | 0.44 |
| <i>RARB</i> | AB188354 ^b | 1092 | 0.01 | 0.35 | 0.01 | 0.40 |
| <i>RARG</i> | AB188355 ^b | 843 | 0.04 | 1.94 | 0.05 | 0.54 |
| <i>MYOD1</i> | AB188356 ^b | 600 | 0.05 | 1.02 | 0.06 | 0.64 |
| <i>GLI2</i> | AB188357 ^b | 1125 | 0.04 | 0.68 | 0.04 | 0.72 |
| <i>GLI3</i> | AB188358 ^b | 324 | 0.00 | 0.41 | 0.00 | 0.42 |
| <i>SP5</i> | AB124563 | 1098 ^c | 0.04 | 1.44 | 0.05 | 0.50 |
| <i>SHH</i> | AB181135 | 564 | 0.01 | 0.49 | 0.01 | 0.33 |
| <i>IHH</i> | AB188359 ^b | 477 | 0.06 | 1.15 | 0.07 | 0.41 |
| <i>FGF8</i> | AB124574 | 465 | 0.02 | 0.43 | 0.02 | 0.23 |
| <i>FGF10</i> | AB124573 | 579 ^c | 0.02 | 0.34 | 0.02 | 0.38 |
| <i>WNT2B</i> | AB188360 ^b | 936 | 0.02 | 1.54 | 0.02 | 0.71 |
| <i>WNT3A</i> | AB188361 ^b | 813 | 0.01 | 0.99 | 0.01 | 0.81 |
| <i>WNT4</i> | AB188362 ^b | 408 | 0.03 | 1.06 | 0.03 | 0.52 |
| <i>WNT5A</i> | AB188363 ^b | 828 | 0.02 | 1.00 | 0.02 | 0.91 |
| <i>WNT7A</i> | AB188364 ^b | 822 | 0.00 | 0.81 | 0.00 | 0.93 |
| <i>WNT8A</i> | AB188365 ^b | 936 | 0.07 | 1.68 | 0.09 | 1.08 |
| <i>WNT11</i> | AB188366 ^b | 408 | 0.01 | 0.97 | 0.02 | 0.79 |
| <i>BMP2</i> | AB181137 | 651 | 0.07 | 0.34 | 0.07 | 0.40 |
| <i>BMP4</i> | AB181138 | 885 | 0.08 | 0.92 | 0.09 | 0.57 |
| <i>BMP7</i> | AB188367 ^b | 663 | 0.01 | 1.10 | 0.01 | 1.40 |
| <i>LFNG</i> | AB188368 ^b | 771 | 0.02 | 1.42 | 0.03 | 0.94 |
| <i>RFNG</i> | AB188369 ^b | 771 | 0.04 | 0.67 | 0.05 | 0.80 |
| <i>MFNG</i> | AB188370 ^b | 657 | 0.12 | 0.96 | 0.13 | 0.77 |
| <i>FGFR1</i> | AB188371 ^b | 597 | 0.05 | 1.55 | 0.06 | 0.48 |
| <i>FGFR2</i> | AB188372 ^b | 981 | 0.00 | 0.53 | 0.00 | 0.63 |
| <i>FGFR4</i> | AB188373 ^b | 750 | 0.04 | 1.79 | 0.06 | 0.57 |
| <i>APCDD1</i> | AB124565 | 1545 ^c | 0.05 | 0.87 | 0.05 | 1.06 |
| <i>CRABP1</i> | AB124564 | 411 ^c | 0.02 | 0.46 | 0.02 | 0.46 |
| <i>CTNNB1</i> | AB124575 | 2346 ^c | 0.00 | 0.55 | 0.00 | 0.61 |
| <i>CDH1</i> | AB188374 ^b | 1917 | 0.19 | 3.31 | 0.23 | 0.75 |
| <i>GAPD</i> | AB124567 | 1023 ^c | 0.06 | 0.65 | 0.06 | 0.63 |
| <i>EEF1A1</i> | AB124568 | 1386 ^c | 0.00 | 0.58 | 0.00 | 0.61 |
| <i>LDHA</i> | AF363794 | 996 ^c | 0.06 | 0.63 | 0.06 | 0.75 |
| <i>LDHB</i> | AF363795 | 1002 ^c | 0.05 | 0.79 | 0.05 | 0.84 |
| <i>THOC2</i> | AB188375 ^b | 891 ^c | 0.01 | 0.65 | 0.01 | 0.76 |
| <i>PLP1</i> | AF369033 | 555 ^c | 0.04 | 0.90 | 0.05 | 0.55 |
| <i>RAG2</i> | AF369089 | 1476 ^c | 0.11 | 0.86 | 0.05 | 0.55 |
| <i>GHR</i> | AF211173 | 1806 ^c | 0.16 | 0.60 | 0.15 | 0.65 |
| <i>TSHB</i> | AY618874 | 402 ^c | 0.11 | 0.94 | 0.11 | 0.98 |
| <i>PRNP</i> | AB088368 | 765 ^c | 0.39 | 1.87 | 0.39 | 1.76 |
| <i>TYR</i> | AB024280 | 1569 ^c | 0.10 | 0.84 | 0.10 | 0.91 |
| <i>RPL23</i> | AB188376 ^b | 315 ^c | 0.00 | 0.78 | 0.00 | 0.74 |
| <i>RPL30</i> | AB188378 ^b | 345 ^c | 0.00 | 0.53 | 0.00 | 0.61 |
| <i>RPS20</i> | AB188377 ^b | 354 ^c | 0.00 | 0.57 | 0.00 | 0.64 |

Sequences of chicken orthologs were retrieved from Ensembl.^aGene symbols designated for human orthologs are indicated. ^bSequenced in this study. ^cContains a whole coding sequence. ^dNumbers of synonymous and non-synonymous substitutions were estimated with the method of Nei and Gojobori (1985). ML, maximum likelihood.

Table 4. Gene mapping on *P. sinensis* chromosomes

| Gene symbol ^a | <i>P. sinensis</i> | | Chromosomal location of orthologs | | |
|--------------------------|-----------------------|-----------|-----------------------------------|--------------------|--------------------|
| | Acc. No. | Location | Chicken | Human ^g | Mouse ^g |
| <i>MFNG</i> | AB188370 ^b | 1p | 1 ^f | 22q13.1 | 15qE2 |
| <i>WNT11</i> | AB188366 ^b | 1q | 1 ^d | 11q13.5 | 7qF1 |
| <i>RARB</i> | AB188354 ^b | 2p | 2 ^f | 3p24.2 | 14qA2 |
| <i>SHH</i> | AB181135 | 2p | 2p ^c | 7q36.3 | 5qA3 |
| <i>APCDD1</i> | AB124565 | 2q | 2q ^c | 18q11.22 | 18qD3 |
| <i>BMP2</i> | AB181137 | 3p | 3 ^e | 20p12.3 | 2qF3 |
| <i>MSX1</i> | AB124572 | 4q | 4 ^f | 4p16.2 | 5qB2 |
| <i>LEF1</i> | AB124566 | 4q | 4q ^c | 4q25 | 3qH1 |
| <i>MYOD1</i> | AB188356 ^b | 5p | 5q ^d | 11p15.1 | 7qB3 |
| <i>BMP4</i> | AB181138 | 5q | 5 ^e | 14q22.2 | 14qC1 |
| <i>PAX9</i> | AB181136 | 5q | 5q ^c | 14q13.3 | 12qC2 |
| <i>PRRX1</i> | AB188347 ^b | 5q | 8 ^f | 1q32.3 | 1qH1 |
| <i>FGF10</i> | AB124573 | 6q | Z ^f | 5p12 | 13qD23 |
| <i>HOXD13</i> | AB188346 ^b | MIC(7q) | 7q ^c | 2q31.1 | 2qC3 |
| <i>SP5</i> | AB124563 | MIC(7q) | 7q ^c | 2q31.1 | 2qC3 |
| <i>EN1</i> | AB188348 ^b | MIC(7q) | 7 ^f | 2q14.2 | 1qE2 |
| <i>GLI2</i> | AB188357 ^b | MIC(7q) | 7q ^c | 2q14.2 | 1qE2 |
| <i>FGF8</i> | AB124574 | MIC(8-10) | 6 ^f | 10q24.32 | 19qD1 |
| <i>FGFR2</i> | AB188372 ^b | MIC(8-10) | 6 ^f | 10q26.13 | 7 (63.0 cM) |
| <i>EMX2</i> | AB188349 ^b | MIC(8-10) | 6 ^f | 10q26.11 | 19qD3 |
| <i>PAX3</i> | AB188350 ^b | MIC(8-10) | 9 ^f | 2q35-q37 | 1 (44.0 cM) |
| <i>CRABP1</i> | AB124564 | MIC(11-) | 10 ^f | 15q25.1 | 9qC |
| <i>DDX46</i> | AB188384 ^b | MIC(11-) | 13 ^f | 5q31.1 | 13 (B1) |
| <i>WNT2B</i> | AB188360 ^b | MIC(11-) | 26 ^f | 1p13.2 | 3qF3 |
| <i>SKI</i> | AB188380 ^b | MIC(11-) | 21 ^f | 1p36.33 | 4qE2 |
| <i>PAX7</i> | AB188351 ^b | MIC(11-) | 21 ^f | 1p36.13 | 4qD3 |
| <i>LFNG</i> | AB188368 ^b | MIC(11-) | 14 ^f | 7p22.3 | 5qG1 |
| <i>TWIST2</i> | AB188379 ^b | MIC(11-) | 7 ^f | 2q37.3 | 1 D |
| <i>BMP7</i> | AB188367 ^b | MIC(11-) | 20 ^f | 20q13.31 | 2qH3 |
| <i>WNT7A</i> | AB188364 ^b | MIC(11-) | 12 ^f | 3p25.1 | 6qD2 |
| <i>WNT5A</i> | AB188363 ^b | MIC(11-) | 12 ^f | 3p14.3 | 14qB |

^aGene names were indicated as gene symbols designated for human orthologs.

^bSequenced in this study. ^cMapped with FISH in this study. ^dSuzuki *et al.* (1999).

^eGuttenbach *et al.* (2000). ^fMapped *in silico* in this study. ^gMapping information on mouse and human chromosomes were retrieved from NCBI Entrez Gene. MIC, microchromosome. Number of distinguishable microchromosomes and its arm (7q, 8-10, and 11-) are indicated in parentheses.